MOLECULAR PHYSICS, 1996, VOL. 88, NO. 6, 1575–1602

Understanding the critical properties of chain molecules

By CARLOS VEGA and LUIS G. MACDOWELL
Departamento de Química Física, Facultad de Ciencias Químicas, Universidad Complutense, 28040 Madrid, Spain

(*Received 9 November 1995; revised version accepted 20 February 1995*)

The vapour–liquid equilibrium of n-alkanes is computed from a simple perturbation theory. A very accurate equation of state for the repulsive n-alkane chain is combined with a mean-field term which accounts for the contribution of attractive forces to the free energy. The theory correctly predicts the existence of a maximum in the critical density of n-alkanes. When differences in the energetic interactions between methane, methyl and methylene groups are included, a maximum in the critical pressure is found for ethane, in good agreement with experiment. The simplicity of the perturbation scheme allows for an analysis of the conditions that a chain model should possess in order to present maxima either in critical density or pressure. It is shown that the conditions needed for the existence of a maximum in the critical density are (1) overlaps between contiguous sites and (2) small differences in mass between monomer, exterior and interior sites. The conditions needed for the existence of a maximum in the critical pressure are (1) overlaps between contiguous sites and (2) small differences between the energy parameters of the monomer, exterior and interior sites. The presence of flexibility is not a requirement for the existence of maxima in the critical density or pressure and therefore rigid models may also exhibit them. The proposed theory, whereas quite simple, contains the minimum number of ingredients to explain the appearance of maxima in the critical density or pressure of n-alkanes and of more general chain models.

1. Introduction

n-Alkanes are compounds of great interest for the chemical industry and a number of their thermophysical properties have been determined experimentally. For instance, the vapour–liquid equilibria and critical properties of low molecular weight n-alkanes are relatively well known [1, 2]. This is not the case for the higher homologues of the series, for which the experimental critical properties are not available. This is due to the fact that n-alkanes are thermally unstable for temperatures higher than $T = 650$ K, so that their critical point cannot be reached before they decompose. However, most of the predictions used in chemical engineering use the corresponding states principle and therefore require a previous knowledge of the critical properties of the compound under consideration.

Recently, there has been some progress in the estimate of the critical properties of n-alkanes. First, the critical properties of long n-alkanes have been determined by Smith *et al.* [3] and Anselme *et al.* [4]. These authors analysed the chemical decomposition of n-alkanes at high temperatures, and were able to estimate the critical properties of long n-alkanes. A very interesting conclusion of the study of Anselme *et al.* [4] is the presence of a maximum in the critical density when plotted versus the number of carbons of the molecule. That was surprising since most of the previous estimates of the critical density suggest that it reaches an asymptotic value for high weight n-alkanes [5]. Secondly, Siepmann, Karaborni and Smit have used computer

0026–8976/96 $12·00 © 1996 Taylor & Francis Ltd

simulation to estimate the critical properties [6, 7] of n-alkanes. They used the so-called Gibbs ensemble, which allows for the determination of the vapour–liquid equilibria of a given molecular model [8]. The work of Siepmann *et al.* [6] and of Smit *et al.* [7] again confirms the presence of a maximum in the critical density of n-alkanes. Therefore, the maximum in the critical density of n-alkanes has been so far confirmed both by experimental work and by computer simulation.

In the last 15 years a great amount of work has been devoted to the study of flexible models. A number of simulation [9–17] and theoretical [18–32] studies have appeared dealing with the determination of the equation of state (EOS) of repulsive flexible models. Within this field of research, we have recently proposed an EOS for repulsive n-alkane models [33–35]. It has been shown that the proposed EOS yields very good agreement with simulation results.

The study of repulsive flexible models is of great interest since they can be taken as the reference system in perturbative treatments of flexible molecules. In perturbative treatments, the EOS and structure of the reference system must be known. In this work, the vapour–liquid equilibria of n-alkanes will be determined from perturbation theory. For the reference system we shall use the very accurate EOS recently proposed by us [35]. The perturbation term will be evaluated within the mean-field approximation [36]. The goal of this paper is to show that the maximum of the critical density for n-alkanes found in experimental and simulation studies can be explained by a quite simple theory. In addition, the maximum in the critical pressure of n-alkanes which appears for ethane will also be explained. The simplicity of the theory will allow for an analysis of the requirements that a chain model should possess in order to present maxima either in the critical density or pressure.

The outline of this paper is as follows. In section 2, the perturbation theory used for the calculation of the vapour–liquid equilibria of n-alkanes will be described. In section 3, critical properties obtained from this theory will be compared with the experimental results. In section 4, the theory will be applied to a general chain model and the conditions for the appearance of maxima in critical density or pressure will be established. In section 5, the main conclusions to this work are presented.

2. Mean-field theory for n-alkanes

We shall start by describing the n-alkane model used in this work. We shall use the united atom approach so that methylene (CH_2) and methyl (CH_3) groups are described by an interaction site located on the position of the carbon atom. The n-alkane is therefore described by n interaction sites, where n is the number of carbon atoms. The geometry of the n-alkane is defined by the C–C distance which is taken as $l = 1{\cdot}53$ Å, the bond angle, $\theta = 109{\cdot}5°$, and the torsional degrees of freedom. We shall use the rotational isomeric state (RIS) approximation [37] so that we regard the n-alkane as a multicomponent mixture. The total energy U_T of the system, (excluding the kinetic energy) is given by a intramolecular U_{intra} and an intermolecular U_{inter} part:

$$U_T = U_{intra} + U_{inter}. \tag{1}$$

The non-bonded interactions between sites of different molecules or between sites of the same molecule that are more than three bonds apart are described by the Lennard–Jones (LJ) potential, which is given by

$$u(r_{ij}) = 4\varepsilon_{ij}[(\sigma/r_{ij})^{12} - (\sigma/r_{ij})^{6}] \tag{2}$$

where σ is the diameter of the site and ε_{ij} is the energy interaction between sites i and

Table 1. Values of interaction energies ε between methane molecules, methyl groups and methylene groups used in this work. Two different models denoted as the HETA and HOMA were used. Values of ε for the HETA model were taken from [38, 39] except that for methane which was obtained by fitting the second virial coefficient of a Lennard–Jones model to the experimental second virial coefficient of methane as reported in [61]. In the HOMA model the value of ε is arbitrarily set to that of the CH_2–CH_2 group for all types of interactions.

Interaction	HETA (ε/k)/K	HOMA (ε/k)/K
CH_4–CH_4	146	49·7
CH_3–CH_3	104	49·7
CH_2–CH_2	49·7	49·7
CH_3–CH_2	71·89	49·7

j, a distance r_{ij} apart. The sites of the chain will be labelled such that one of the methyl groups has $i = 1$ and the other one has $i = n$.

Let us now describe the intramolecular contribution to the total energy. For methane, ethane and propane there is no intramolecular contribution to the total energy of the system. For longer chains the intramolecular energy u_{intra} of a given molecule is given by

$$u_{\text{intra}} = cD + \sum_{i=1}^{n-4} \sum_{j=i+4}^{n} 4\varepsilon_{ij}[(\sigma/r_{ij})^{12} - (\sigma/r_{ij})^{6}] \tag{3}$$

In equation (3), the number of *gauche* bonds of the molecule is denoted as c and the energy of a *gauche* bond with respect to that of a *trans* bond is denoted as D. The value of D is computed from equation (14) of [33] using the torsional potential described by Ryckaert and Bellemans [9]. The total intramolecular energy U_{intra} of the system is obtained by summing u_{intra} over all the molecules of the system.

The intermolecular energy between a pair of molecules is obtained as

$$u_{\text{inter}} = \sum_{i=1}^{n} \sum_{j=1}^{n} 4\varepsilon_{ij}[(\sigma/r_{ij})^{12} - (\sigma/r_{ij})^{6}] \tag{4}$$

where here i and j correspond to sites located on different molecules. The total intermolecular energy U_{inter} is obtained by summing u_{inter} over all the pairs of molecules of the system. As it can be seen from equations (3) and (4), the LJ potential is used for describing intramolecular and intermolecular interactions. In this work, the parameter σ is set to $\sigma = 3{\cdot}923$ Å in all the calculations involving n-alkanes.

Two different models of n-alkane will be considered. In the heterogeneous alkane model (HETA), the energy parameters of the CH_4, CH_3 and CH_2 groups will be different, whereas in the homogeneous alkane model (HOMA), they will be set to the same value. In table 1 the values of ε for the HETA and HOMA models are given. The set of ε of the HETA model correctly describes [38, 39] the experimental second virial coefficients of n-alkanes.

In order to obtain the thermodynamic properties of the system described by equations (1)–(4), we shall use perturbation theory. Each site–site interaction will be

split into a reference part and a perturbation part. The Weeks–Chandler–Andersen (WCA) [40] choice of the reference system will be used here. Accordingly, the reference system is described by a site–site interaction, u_0, given by

$$u_0(r_{ij}) = 4\varepsilon_{ij}[(\sigma/r_{ij})^{12} - (\sigma/r_{ij})^6] + \varepsilon_{ij} \quad r_{ij} < 2^{1/6}\sigma, \tag{5}$$

$$u_0(r_{ij}) = 0 \quad r_{ij} > 2^{1/6}\sigma. \tag{6}$$

The perturbation part of the potential, $u_1(r_{ij})$, is defined as

$$u_1(r_{ij}) = u(r_{ij}) - u_0(r_{ij}). \tag{7}$$

The total energy of a given configuration of the reference system is given by equations (1)–(4) with u replaced by u_0. The torsional contribution to the total energy is therefore included into the reference system.

We shall use first-order perturbation theory so that the residual Helmholtz free energy A of the system is given by

$$A = A_0 + A_1, \tag{8}$$

where A_0 is the residual free energy of the reference system and A_1 is the perturbation term.

Recently, we have proposed a procedure for obtaining the EOS and free energy of repulsive WCA n-alkane models. It has been shown that the proposed equation yields very good agreement with simulation data. The compressibility factor of the reference system, $Z_0 = p_0/(\rho kT)$, and its residual free energy A_0 will be obtained as

$$A_0/NkT = 2(\alpha - 1)\ln\left[\frac{2(1-y)^3}{(2-y)}\right] - \frac{(2\alpha - 1)(2y-3)}{(1-y)^2} - 3(2\alpha - 1) \tag{9}$$

$$Z_0 = (2\alpha - 1)\left[\frac{(1+y+y^2-y^3)}{(1-y)^3}\right] - (2\alpha - 2)\left[\frac{(1+y-y^2/2)}{(1-y)(1-y/2)}\right] \tag{10}$$

$$y = \rho V_m, \tag{11}$$

where N is the number of molecules, V the total volume and $\rho = N/V$ the number density of the system. The packing fraction y is defined in equation (11), where V_m is the molecular volume. We shall use Wertheim's [19, 20] EOS (equation (10)) to describe the repulsive WCA n-alkane, with the parameter m of the original theory replaced by $(2\alpha - 1)$, where α is the non-sphericity of the n-alkane model. The origin of this replacement is as follows. Wertheim's EOS was derived for a fluid made up of m tangent hard spheres. The second virial coefficient obtained from Wertheim's EOS for m tangent hard spheres is given by [23]

$$B_2/V_m = 1{\cdot}5m + 2{\cdot}5. \tag{12}$$

The non-sphericity parameter will be defined as [41]

$$B_2/V_m = 1 + 3\alpha, \tag{13}$$

where B_2 is the second virial coefficient of the hard model. By equating equations (12) and (13), one obtains

$$m = 2\alpha - 1. \tag{14}$$

Therefore we shall use Wertheim's EOS with m replaced by $(2\alpha - 1)$. Note that non-integer values of m are now allowed since there is no reason why α should be an integer.

Therefore a hard-chain model made up of n monomer units (n is an integer) is described with Wertheim's EOS by using m *effective* tangent hard spheres (m is not necessarily an integer). The modification of Wertheim's EOS given by equation (10) allows the study of chains in which overlapping between bonded monomers is allowed. The replacement described by equation (14) has no advantage unless a way of estimating the second virial coefficient of the model is available (so that α and m can be obtained from equations (13) and (14)). The evaluation of α is difficult since it requires a knowledge of the second virial coefficient, which is quite often unknown. However, a good estimate can be obtained by using convex body geometry, so that it is approximated as [42, 43]

$$\alpha \simeq (R_m S_m)/(3V_m), \tag{15}$$

where S_m is the area of the molecular surface and R_m is the mean radius of curvature. Equation (15) is exact for convex bodies (those in which any line segment connecting two points of the body is fully contained inside the body) so that equation (15) and equation (13) yield identical values of α. For non-convex bodies, equation (15) is only an approximation to the true value defined by equation (13). When using equation (15) for non-convex bodies, R_m is usually taken from a convex body of similar shape to the molecule under consideration. For a flexible non-convex model, the non-sphericity of each conformer can be approximated by equation (15) and the non-sphericity of the molecule is defined as the weighted averaged of the non-sphericities of the different possible conformers of the molecule. The non-sphericity parameter takes the value of one for a sphere and a value larger than one for non-spherical models. In Appendix A we provide a way of estimating α and V_m for hard n-alkane models. The basic idea is to compute them for the different conformers of the n-alkane and to perform a weighted average. Here, we shall assume that values of α and V_m are available for the hard n-alkane models considered and we refer the reader to Appendix A and to [35] for further details. In Appendix A, empirical fits which describe the variation of α and V_m with T and n are given for the HOMA and HETA models.

The first-order perturbation term A_1 can be divided into an intramolecular contribution A_1^{intra} and an intermolecular contribution A_1^{inter} so that

$$A_1^{intra}/N = \rho \sum_{i=1}^{n-4} \sum_{j=i+4}^{n} \int u_1(r_{ij})\, g'_{0,ij}(r_{ij})\, 4\pi r_{ij}^2 \mathrm{d}r_{ij} \tag{16}$$

$$A_1^{inter}/N = \rho/2 \sum_{i=1}^{n} \sum_{j=1}^{n} \int u_1(r_{ij})\, g_{0,ij}(r_{ij})\, 4\pi r_{ij}^2 \mathrm{d}r_{ij} \tag{17}$$

where $g'_{0,ij}$ is the intramolecular pair correlation function of the reference system between sites i and j, and $g_{0,ij}$ is the intermolecular pair correlation of the reference system between sites i and j. We follow the notation of [44] for defining intra- and intermolecular correlation functions. The functions $g_{0,ij}$ and $g'_{0,ij}$ present different behaviour. For instance, at any density, $g_{0,ij}$ goes to one for sufficiently large values of r_{ij}, whereas $g'_{0,ij}$ goes to zero. To give another example, for sufficiently low density $g_{0,ij}$ is close to one for values of r outside the hard core, whereas the function $g'_{0,ij}$ behaves as a Gaussian-like curve even at zero density. The different behaviour of $g'_{0,ij}$ and $g_{0,ij}$ means that whereas A_1^{intra} is different from zero even at zero density, A_1^{inter} is zero at zero density. It has been shown previously that for n-alkane models at a given temperature, changes in conformational population with density are small [33, 34, 45].

Accordingly, A_1^{intra} is approximately constant for a given temperature. In this work it is assumed that A_1^{intra} is an arbitrary function of T, but independent of density, whose explicit form is irrelevant to the vapour–liquid equilibrium calculations. In order to obtain A_1^{inter}, the mean-field approximation will be used so that $g_{0,ij}$ will be given by:

$$g_{0,ij} = 0 \quad r_{ij} < \sigma \tag{18}$$

$$g_{0,ij} = 1 \quad r_{ij} > \sigma \tag{19}$$

Of course, more elaborate choices of $g_{0,ij}$ are possible [25, 29, 44, 46] but in this work we wish to keep the calculations as simple as possible. When equations (18) and (19) are substituted in equation (17), one obtains for the A_1 contribution (without including the constant $A_1^{\text{intra}}(T)$):

$$A_1/N = -\rho^* \left(\frac{10\pi\sqrt{2}}{9} + \frac{2\pi(\sqrt{2}-1)}{3} \right) \varepsilon_T \tag{20}$$

$$\varepsilon_T = \delta_{n,1}\varepsilon_{CH_4\text{-}CH_4} + (1-\delta_{n,1})(4\varepsilon_{CH_3\text{-}CH_3} + (n-2)^2\varepsilon_{CH_2\text{-}CH_2} + 4(n-2)\varepsilon_{CH_3\text{-}CH_2}) \tag{21}$$

where we have defined the reduced number density ρ^* as $\rho^* = \rho\sigma^3$. The function $\delta_{i,j}$ in equation (21) is the Kroenecker delta function which is used here to keep equation (20) in a general form valid for any n-alkane. In what follows, the parentheses in equation (20) will be replaced by its numerical value, which is equal to 5·804 06. The factors, 4, $(n-2)^2$ and $4(n-2)$ appearing on the right-hand side of equation (21) are due to the fact that there are four methyl–methyl interactions, $(n-2)^2$ methylene–methylene interactions and $4(n-2)$ methyl–methylene interactions between a pair of n-alkane molecules for $n > 1$. One may be tempted to treat the intra- and intermolecular interactions within the mean-field approximation. The number of intramolecular interactions grows approximately as $N(n)(n-1)/2$, whereas the number of intermolecular interactions grows as $N(N-1)n^2/2$. In the thermodynamic limit (N infinity), the number of intramolecular interactions becomes arbitrarily small when compared to the number of intermolecular interactions. In other words, to treat intramolecular and intermolecular interactions within the mean-field approximation means that A_1^{intra} is set to zero. This is incorrect since even at zero density A_1^{intra} is different from zero. In this work we assume that A_1^{intra} is not zero but constant for a given temperature. Although for the purpose of vapour–liquid calculations there is no difference between setting A_1^{intra} to a constant which depends on temperature only or setting it to zero, these two approaches are conceptually different.

The total free energy A_T of the system is obtained by adding the residual free energy A to the ideal contribution. This ideal contribution has three different terms, a purely kinetic term which depends on density (i.e., $\ln(\rho^*) - 1$) and two other terms (see equation (21) of [33]), one of which is of entropic origin while the other is an intramolecular energy. Since in this work changes in the population of conformers with density are neglected, only the $\ln(\rho^*)$ is relevant for phase equilibria calculations. Accordingly, the final expression for A_T is

$$A_T/NkT = 2(\alpha-1)\ln\left[\frac{2(1-y)^3}{(2-y)}\right] - \frac{(2\alpha-1)(2y-3)}{(1-y)^2} - 3(2\alpha-1) - 5{\cdot}804\,06\rho^*\varepsilon_T/(kT) + \ln(\rho^*) - 1, \tag{22}$$

Equation (22) is valid for both the HOMA and HETA models. The only difference is

the value of ε_T (see equation (21) and table 1) and the slight differences in α and V_m for a given n and T (see the empirical fits given in Appendix A). The compressibility factor Z of the system is obtained by differentiating the free energy with respect to the density, so that one obtains

$$Z = Z_0 - 5{\cdot}804\,06\rho^*\varepsilon_T/(kT), \tag{23}$$

where Z_0 is the compressibility factor of the reference system, given by equation (10). The vapour–liquid equilibrium of the model is obtained by equating the chemical potential and pressure of the vapour and liquid phases. By using equations (22) and (23), the vapour–liquid equilibrium of n-alkanes from methane (n = 1) up to n = 48 has been computed.

To summarize, in this section a first-order perturbation theory is developed with an accurate description of the WCA reference system and with attractive forces considered within the mean-field approximation. The proposed theory, which combines Wertheim's EOS for the reference system and a mean-field term, is similar to that used in previous studies [20, 47]. The main difference is that, in this work, the parameter m appearing in Wertheim's EOS is related to the non-sphericity α so that it can be determined for models which contain overlapping hard spheres, as is the case for n-alkane models. Due to the mean-field approximation, we do not expect quantitative agreement between the proposed theory and either experiment or simulation. Eventually, the mean-field approximation could be removed as illustrated in [48]. However, the main purpose of this work is to check if the main features of the critical properties of n-alkanes can be reproduced by a simple theoretical model.

3. Critical properties of n-alkanes

We shall start by presenting the results obtained for the HETA model. In this model, methane, methyl and methylene differ in their interaction energies, which were chosen to reproduce the second virial coefficient of n-alkanes from methane up to n-hexadecane [38, 39]. Table 2 presents the critical properties as estimated from the perturbation theory of this work. In figure 1, a comparison between theoretical and experimental critical temperatures is made. As can be seen from figure 1, the critical temperature increases with the length n of the chain. For short n-alkanes the theory underpredicts the critical temperature, whereas for long n-alkanes it overestimates it. This is mainly due to the fact that the mean-field approximation, $g(r) = 1$, underestimates the contact value of the site–site distribution for short chains and overestimates it for long chains.

In figure 2, theoretical critical pressures are compared with experimental ones. For short n-alkanes the critical pressure is underpredicted, whereas the opposite is true for long n-alkanes. This is a consequence of the errors of the theory in predicting the critical temperature, as previously discussed. The theory predicts a maximum in the critical pressure of n-alkanes which is located in ethane and this is in good agreement with experiment. This is remarkable since other studies concerning vapour–liquid equilibria of n-alkanes were unable to find this maximum [47].

We shall now consider the critical density. In table 2, the reduced number density at the critical point ρ_c^* is given. The critical density d_c is also presented. In order to obtain d_c, it is assumed that the molecular masses of CH_4, CH_3 and CH_2 groups are

Table 2. Critical properties as obtained from perturbation theory for the HETA model of n-alkanes. The number of carbon atoms is denoted as n, T_c is the critical temperature, p_c is the critical pressure. The reduced number density at the critical point is denoted as $\rho_c^* = (N/V_c)\sigma^3$ where V_c is the total volume of the system at the critical point. The critical density d_c is obtained by assigning the molecular weights of 16 g mol^{-1}, 15 g mol^{-1} and 14 g mol^{-1} to the CH_4, CH_3 and CH_2 groups, and d_c' is obtained by assuming that the molecular weights of the CH_4, CH_3 and CH_2 groups are equal to 14.

n	T_c/K	p_c/MPa	ρ_c^*	d_c/g cm^{-3}	d_c'/g cm^{-3}
1	156·86	3·30	0·255 23	0·1123	0·0983
2	303·26	4·34	0·174 67	0·1441	0·1345
3	401·38	4·23	0·128 93	0·1560	0·1489
4	491·75	4·05	0·100 82	0·1608	0·1553
5	575·17	3·85	0·082 12	0·1626	0·1581
6	652·52	3·65	0·068 79	0·1627	0·1589
7	724·61	3·46	0·058 84	0·1618	0·1586
8	792·11	3·29	0·051 16	0·1604	0·1576
10	915·40	2·97	0·040 18	0·1569	0·1547
12	1025·90	2·70	0·032 75	0·1531	0·1513
16	1217·43	2·29	0·023 43	0·1456	0·1443
23	1487·27	1·79	0·015 15	0·1350	0·1342
30	1706·44	1·47	0·010 85	0·1259	0·1253
40	1982·43	1·19	0·007 58	0·1172	0·1168

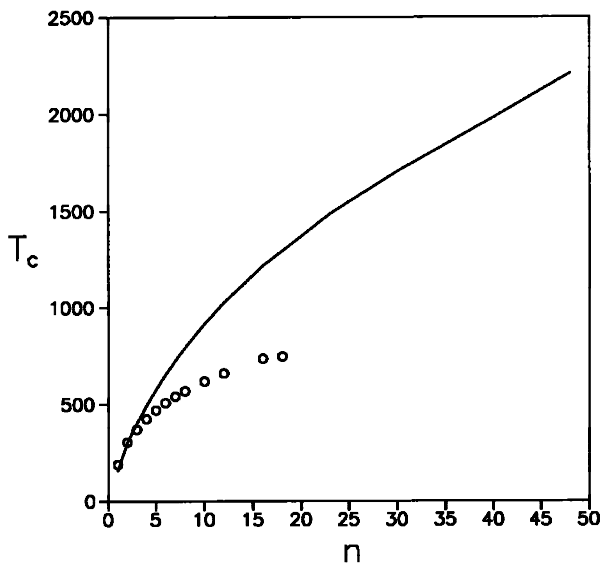

Figure 1. Critical temperature (in Kelvin) of n-alkanes as obtained from the perturbation theory of this work for the HETA model (solid curve). Experimental data (symbols) were taken from [1, 4].

given by 16, 15 and 14 g mol^{-1}, respectively (see fifth column of table 2). In the sixth column of table 2, the critical density is given by assuming that these masses are all equal to 14 g mol^{-1}.

In figure 3, theoretical and experimental critical densities are shown. As can be seen, the critical densities are underestimated by the theory. However, the theory

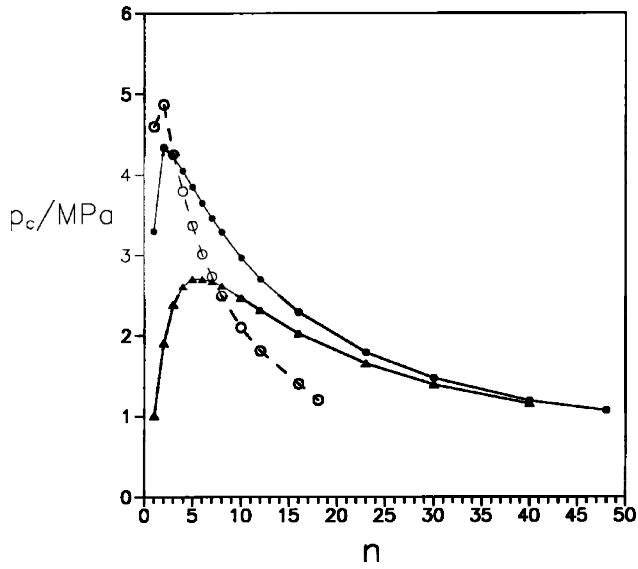

Figure 2. Critical pressures of n-alkanes as obtained from the perturbation theory of this work for the HETA model (solid curve and filled circles) and for the HOMA model (solid curve and filled triangles). Experimental data (dashed curve and open circles) from [1, 4].

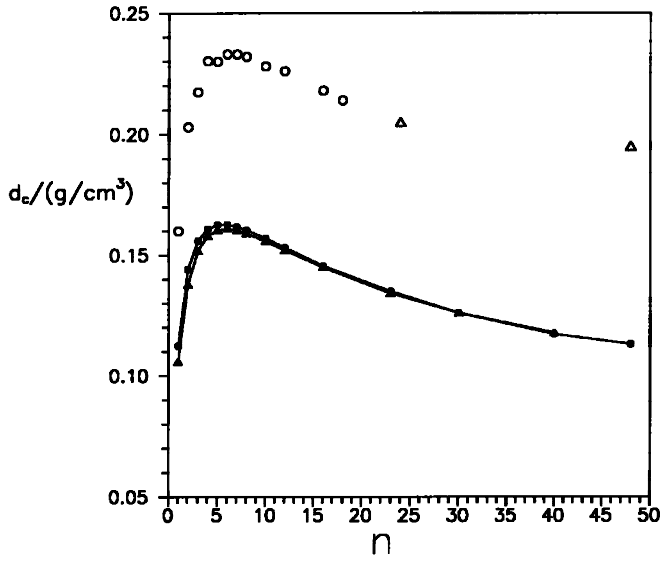

Figure 3. Critical densities of n-alkanes as obtained from the perturbation theory of this work for the HETA model (solid curve and filled circles) and for the HOMA model (solid curve and filled triangles). The molecular weight of CH_4, CH_3 and CH_2 groups was set to 16, 15 and 14 g mol^{-1}, respectively. Experimental data (open circles) from [4]. For C_{48}, the experimental critical density as estimated from Gibbs ensemble simulation from [7] is included.

predicts quite nicely a maximum whose position (i.e., $n = 6$) is in good agreement with experiment. An important conclusion that can be obtained from the results of table 2 is that the presence of this maximum is not due to the different masses of the CH_4, CH_3 and CH_2 groups. When the mass of these groups is set to the same value, it still remains

Table 3. Critical properties obtained from the perturbation theory of this work for the HOMA model of n-alkanes. Rest of the notation as in table 1.

n	T_c/K	p_c/MPa	ρ_c^*	d_c/g cm^{-3}	d_c'/g cm^{-3}
1	50·52	1·00	0·240 56	0·1058	0·0926
2	138·68	1·90	0·167 03	0·1378	0·1286
3	232·06	2·38	0·125 45	0·1518	0·1449
4	322·60	2·61	0·099 01	0·1579	0·1525
5	408·18	2·70	0·081 01	0·1604	0·1559
6	488·53	2·70	0·068 05	0·1609	0·1572
7	563·94	2·67	0·058 31	0·1603	0·1571
8	634·87	2·62	0·050 73	0·1590	0·1563
10	764·99	2·47	0·039 89	0·1558	0·1536
12	882·09	2·32	0·032 52	0·1520	0·1502
16	1085·65	2·02	0·023 32	0·1449	0·1436
23	1373·32	1·65	0·015 05	0·1341	0·1333
30	1607·53	1·39	0·010 86	0·1260	0·1254
40	1909·54	1·15	0·007 62	0·1178	0·1174

(although its position is slightly shifted to longer n-alkanes). To our knowledge, this is the first time that a maximum in the critical density of n-alkanes has been obtained from a theoretical model.

Let us now present the results for the HOMA model. In table 3, the critical properties obtained from perturbation theory are presented. Again, critical temperatures are underpredicted for short n-alkanes and overpredicted for long n-alkanes. The deviation between experimental and theoretical results for short n-alkanes is due not only to the mean-field approximation but also to the use of a small value of ε for the CH_3–CH_3 and CH_4–CH_4 interactions. In figure 2, theoretical critical pressures obtained for this model are presented. It is seen that a maximum in the critical pressure is predicted, but its location ($n = 7$) is shifted considerably with respect to the location of the experimental maximum ($n = 2$). The results of figure 2 illustrate an interesting point. The homopolymer model of n-alkanes (in which all the interaction sites have the same size and interaction energy) presents a maximum in the critical pressure. According to the theory of this work, if CH_4, CH_3 and CH_2 had the same value of ε, then the maximum in the critical pressure would occur for n-heptane. When energy differences between CH_4, CH_3 and CH_2 are introduced, the maximum in the critical pressure is shifted to much shorter chains (i.e., it occurs experimentally for ethane).

Let us now analyse the behaviour of the critical density for the HOMA model. This is shown in table 3 and in figure 3. It is seen that a maximum in the critical density is found for $n = 6$, in good agreement with experiment. The conclusion to be learnt from figure 3 is that the existence of a maximum in the critical density is not due to the differences in energy between CH_4, CH_3 and CH_2 groups, since it is located at exactly the same place (i.e., $n = 6$) for both the HETA and the HOMA models. In table 3, critical densities obtained by assuming that the masses of CH_4, CH_3 and CH_2 are equal are also shown. Again there is a maximum in the critical density and its location is not modified. Therefore, the presence of a maximum in the critical density of n-alkanes is not due to a terminal effect (i.e., differences in the energy interaction or mass between CH_4, CH_3 and CH_2 groups).

In this section we have shown how the HETA model provides a very simple and qualitatively correct understanding of the critical properties of n-alkanes. The

appearance of maxima in the critical density and pressure have been predicted in good agreement with experiment. However, the origin of these maxima is not quite clear. In the next section, we face a more general problem. We try to analyse the geometrical requirements for the existence of a maximum in the critical density or pressure in a chain model.

4. Critical properties of chains

In the previous section it was shown that a simple theory is able to account for the existence of a maximum both in the critical density and pressure of n-alkanes. In this section we shall investigate the geometrical requirements that a chain model should present in order to have maxima in the critical properties when represented as a function of the number n of monomer units. In this section the term chain will be used in a general sense to represent a molecule formed by n units of diameter σ and bond length l. The molecule may be either fully rigid or flexible.

Within the mean-field theory described in section 2, the pressure is obtained from equation (23) as

$$p/(kT/\sigma^3) = \rho^* Z_0 - 5{\cdot}804\,06\rho^{*2}\varepsilon_T/(kT), \tag{24}$$

where Z_0 is given by equation (10) and ε_T is given by

$$\varepsilon_T = \delta_{n,1}\varepsilon_{m\text{-}m} + (1-\delta_{n,1})(4\varepsilon_{e\text{-}e} + (n-2)^2\varepsilon_{i\text{-}i} + 4(n-2)\varepsilon_{e\text{-}i}), \tag{25}$$

where $\varepsilon_{m\text{-}m}$ is the energy parameter between monomer units, $\varepsilon_{e\text{-}e}$ that between extreme sites, $\varepsilon_{i\text{-}i}$ that between interior sites and $\varepsilon_{e\text{-}i}$ that between an extreme and an interior site. Equation (25) is just the translation of equation (21) to a general chain. We shall use the Lorentz–Berthelot rule for $\varepsilon_{e\text{-}i}$ so that $\varepsilon_{m\text{-}m}$, $\varepsilon_{e\text{-}e}$ and $\varepsilon_{i\text{-}i}$ will provide a complete description of the molecular interactions of the model. Equation (24) can be rewritten as

$$p/(kT/\sigma^3) = yZ_0/(V_m/\sigma^3) - 5{\cdot}804\,06y^2\varepsilon_T/(kT(V_m/\sigma^3)^2). \tag{26}$$

The parameters α and V_m depend on the length n of the chain, its geometry and on the temperature T. The temperature dependence of V_m is due to the change with temperature of the hard-core diameter obtained from the Barker and Henderson prescription [49] (see Appendix A). However, the changes of V_m and α with temperature are small [33] and in this section we shall assume that they do not depend on it. Thus, for a given type of chain we consider them a function of n only. The molecular volume will be obtained by assigning a hard diameter equal to σ for each interaction site and computing the volume of the resulting body. We shall now assume that the parameters V_m and α depend on n in a linear form so that they can be expressed as

$$\alpha = 1 + (n-1)c_1 \tag{27}$$

$$V_m^* = V_m/\sigma^3 = \pi/6 + (n-1)c_2. \tag{28}$$

The parameters c_1 and c_2 describe how α and V_m increase with n and they are characteristic of the chain model considered. Equation (27) can be rewritten in terms of m by using equation (14) so that

$$m = 1 + 2(n-1)c_1. \tag{29}$$

Therefore, the parameter c_1 also measures the increase in the *number of effective spheres* m with the number of monomer units n. Although we shall discuss the properties of chain molecules in terms of α and V_m^*, one could use in the discussion the parameters m and V_m^* since α and m are related by equation (14).

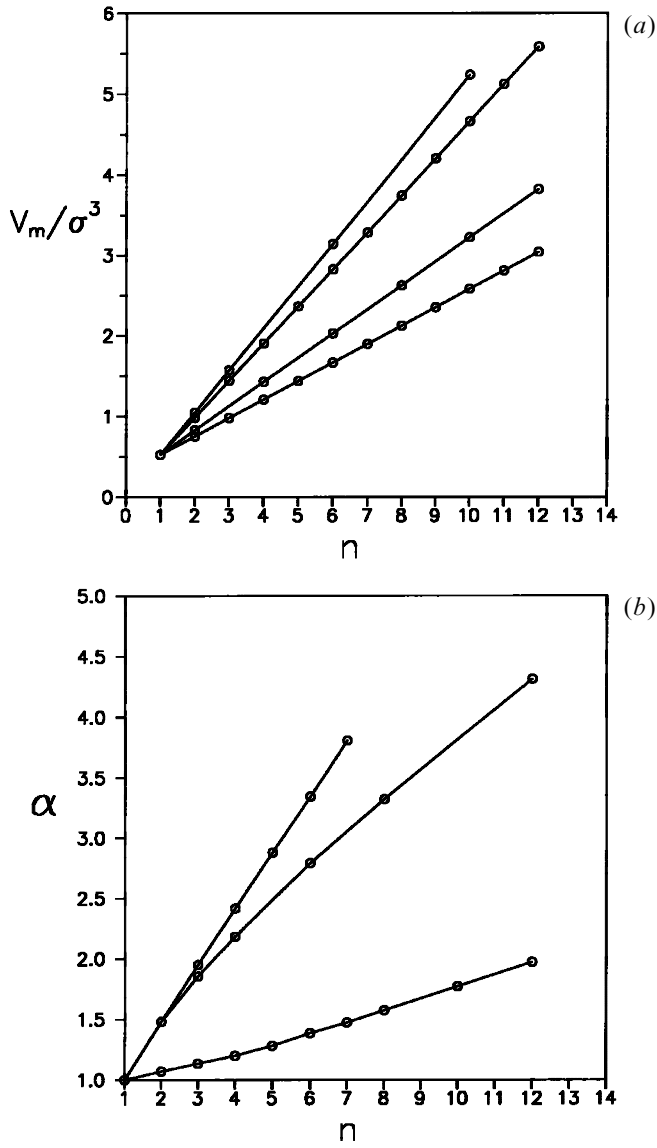

Figure 4. Plot of V_m and α versus n for several chain models. (*a*) Molecular volume, V_m, in σ^3 units, versus n plot. Lines from top to bottom correspond to a chain of tangent hard spheres; a rigid linear chain with reduced bond length $L^* = 0{\cdot}7$; a hard n-alkane model from [35]; and a rigid linear chain with $L^* = 0{\cdot}3$. (*b*) Plot of α versus n. Lines from top to bottom correspond to a rigid linear chain with $L^* = 1$; the pearl necklace model; and the n-alkane model of [35]. The value of α was estimated by using equation (15), except for the pearl necklace model, where equation (13) and the second virial coefficient data from [62] were used.

Let us check the validity of equations (27) and (28). In figure 4(*a*), values of V_m^* versus n are plotted for several chains. It is seen that the behaviour of V_m^* versus n is almost linear for a given type of chain. Moreover, the value of c_2 in equation (28) can be obtained in an approximated manner. In fact, the volume of a given type of chain depends mainly on the reduced bond length and also, to a minor extent, on other

characteristics such as internal bond angles θ or flexibility. If the volume of the chain is approximated by that of a rigid linear chain with the same bond length, the slope of the plot V_m versus n which defines c_2 will be given by

$$c_2 = \pi/12(3L^* - L^{*3}), \tag{30}$$

where $L^* = l/\sigma$ is the reduced bond length. Equation (30) illustrates in an approximate way the geometrical meaning of the parameter c_2 appearing in equation (28).

To evaluate the accuracy of equation (27), the value of α versus n is plotted for different kinds of chains in figure 4 (*b*). It is seen that although α is not a linear function of n, equation (27) can be considered as reasonable for chains that are not too long. For long chains, it has been found that α increases with n (although not always in a linear way). This is an important feature as will be noted later. Therefore, equation (27) is reasonable for short chains, and since c_1 is positive, it captures the increases of α with n that has been observed for long chains. By using equations (27) and (28) in equation (26) and substituting Z_0 (equation (10)), one obtains

$$\begin{aligned} p/(kT/\sigma^3) = {} & y/(\pi/6 + (n-1)\,c_2)\left[(2(1+(n-1)\,c_1) - 1)\frac{(1+y+y^2-y^3)}{(1-y)^3}\right. \\ & \left. - (2(1+(n-1)\,c_1) - 2)\frac{(1+y-y^2/2)}{(1-y)\,(1-y/2)}\right] \\ & - 5{\cdot}804\,06y^2\varepsilon_T/(kT(\pi/6 + (n-1)\,c_2)^2). \end{aligned} \tag{31}$$

The pressure as given by equation (31) is a function of c_1 and c_2, which depend on the geometry of the chain model (i.e., bond length, bond angle, presence or absence of flexibility), the number of monomer units n, and the ratios $k_1 = \varepsilon_{m-m}/\varepsilon_{i-i}$ and $k_2 = \varepsilon_{e-e}/\varepsilon_{i-i}$. For a given set of c_1, c_2, k_1, k_2 and n, the critical properties T_c and y_c can be obtained by setting to zero the first and second derivatives of equation (31) with respect to y at constant T. Once the packing fraction at the critical point y_c is known, the critical density d_c' expressed in units of mass per volume, can be obtained as

$$d_c' = y_c(n/V_m). \tag{32}$$

The use of a prime in equation (32) reminds us that the same mass (in this case an arbitrary value of one) was assigned to the interior and exterior sites. The critical properties for several values of n, with c_1, c_2, k_1 and k_2 fixed, were computed and the presence or absence of a maximum in the critical density or pressure (as a function of n) was established. In this section two models will be considered: the homopolymer chain (HOMP), in which $k_1 = k_2 = 1$, and the heteropolymer chain (HETP), with $k_1 = 3$, $k_2 = 2$.

Before presenting the results for the HOMP and HETP chains, let us discuss the behaviour of the packing fraction at the critical point y_c. The value of y_c computed from equation (26) depends only on α or, with equation (27), on c_1 and n. In figure 5 (*a*), y_c is plotted as a function of α. When α goes to infinity, y_c goes to zero. It can be easily proved that the critical packing fraction computed from equation (26) scales as $\alpha^{-0{\cdot}5}$ for large α (see Appendix B). Figure 5 (*a*) is valid for the HETP and HOMP models, since the value of y_c does not depend either on k_1 or on k_2. In figure 5 (*b*), the compressibility factor at the critical point Z_c is plotted as a function of α. In Appendix B, it is shown that Z_c computed from equation (26) or equation (31) depends on α only and that the asymptotic value of Z_c for large values of α is 1/3.

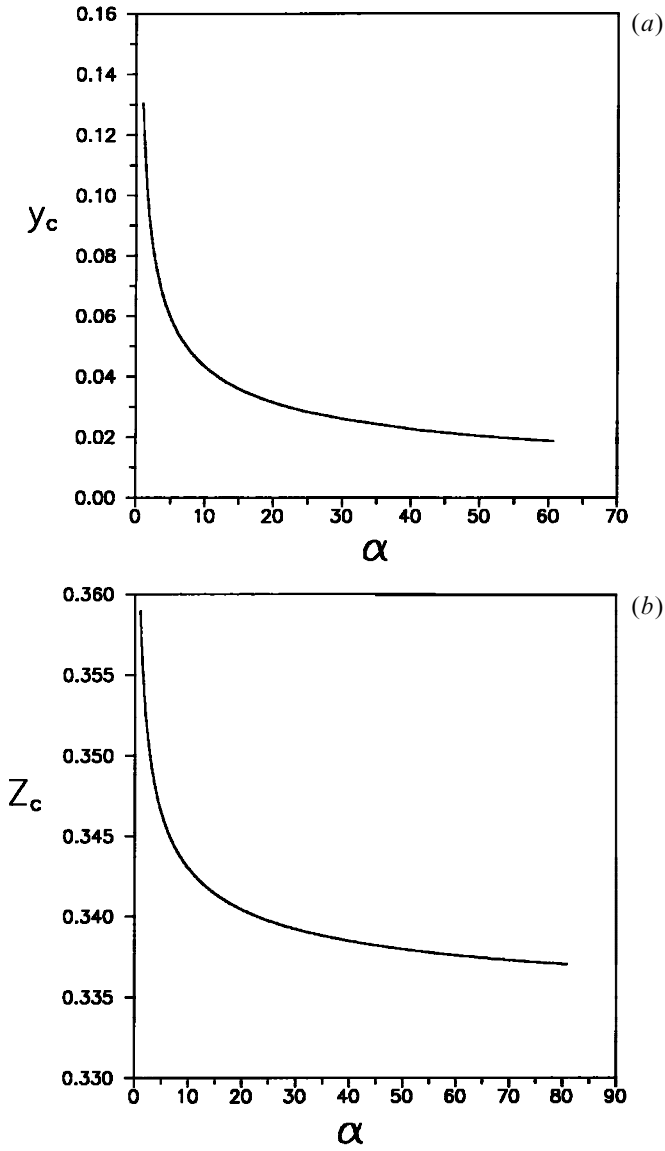

Figure 5. Critical properties obtained from equation (26) as functions of α: (*a*) critical packing fraction y_c: (*b*) compressibility factor at the critical point Z_c.

Let us first discuss the results obtained for the HOMP model. In figure 6(*a*) the behaviour of the critical density as a function of n is depicted for several values of c_1 and c_2. Depending on the value of c_1 and c_2, four different behaviours are found for the critical density. For $c_2 = 0$, the critical density diverges when n goes to infinity. Obviously, the value $c_2 = 0$ has no physical sense, since it means that the molecular volume does not increase with the length of the chain, and this is not possible. When $c_1 = 0$, the critical density reaches an asymptotic and finite value. This means that if the molecule presents a constant value of α regardless of the size of the chain (in this case $\alpha = 1$), an asymptotic critical density is obtained. Obviously, the cases $c_1 = 0$ or $c_2 = 0$ are limiting cases of little interest. In figure 6(*a*), the c_1, c_2 space is divided into

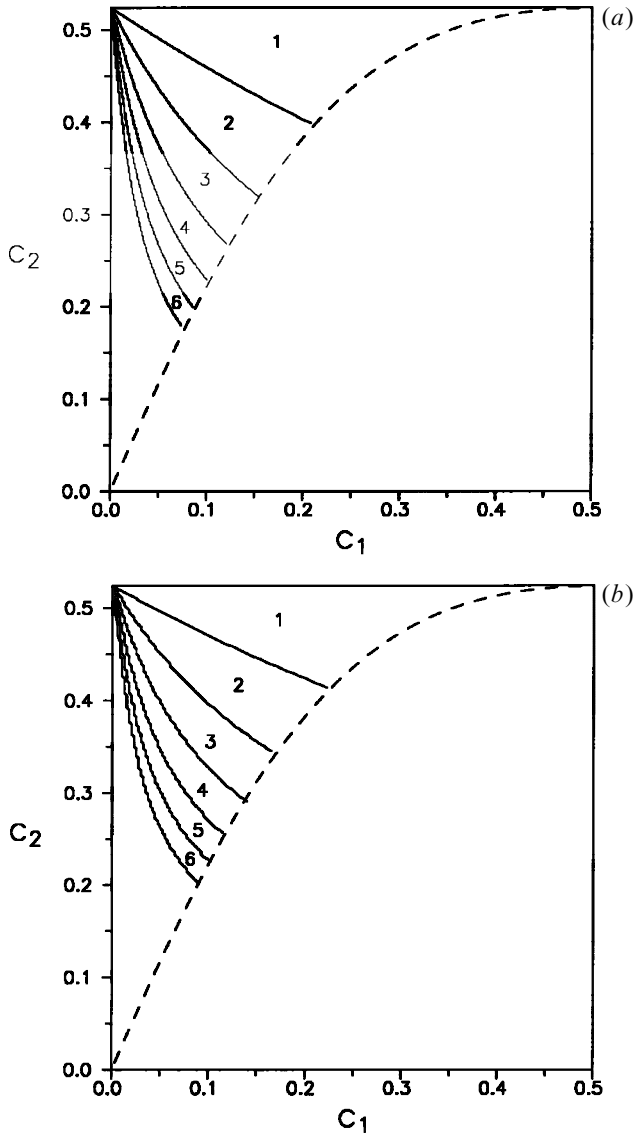

Figure 6. Behaviour of the critical properties as a function of n for the HOMP model (i.e., $k_1 = k_2 = 1$). The number within each region indicates the value of n for which a maximum in the corresponding critical property appears. In the region with no number, the maximum appears for $n > 6$. The dashed curve represents the maximum value of c_1 that can be achieved for a given value of c_2 according to equation (30) and equation (33). (*a*) Results for the critical density; (*b*) results for the critical pressure.

several regions, each of which is labelled by a number. This number represents the value of n for the n-mer at which a maximum appears in the critical density. In the region labelled as 1, the critical density decreases monotonously with n and therefore no maximum in the critical density is found. In the regions labelled with 2, 3, 4, 5, 6, the critical density reaches a maximum for the dimer, trimer, tetramer, pentamer or hexamer respectively, and then decays to zero when n goes to infinity.

In figure 6 (*b*), the behaviour of the critical pressure as a function of n is represented

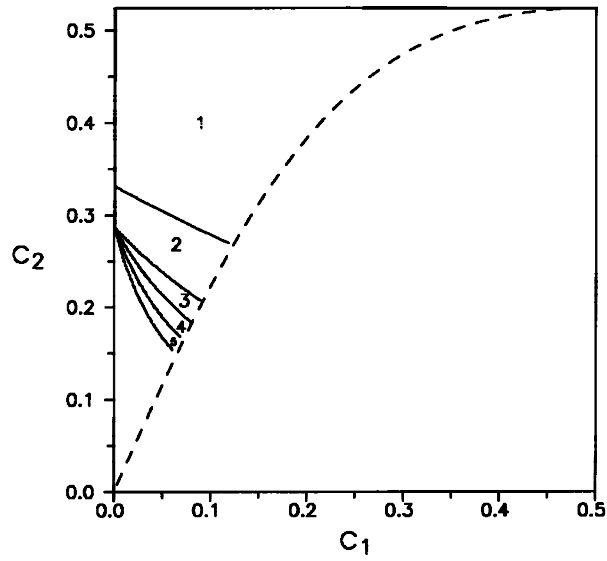

Figure 7. Behaviour of the critical pressure of the HETP with $k_1 = 3$ and $k_2 = 2$ as a function of n. Rest of the notation as in figure 6.

for several c_1, c_2 values. Figure 6(b) is quite similar to figure 6(a). The critical pressure behaves in a similar way to the critical density in the HOMP model. By comparing figure 6(a) to figure 6(b), it may be concluded that when there is a maximum in the critical pressure there is also a maximum in the critical density, appearing at almost the same value of n.

Let us now focus on the HETP with $k_1 = 3$ and $k_2 = 2$. Note that this choice of k_1 and k_2 corresponds approximately with the ratio of ε for n-alkane models presented in the previous section. Critical densities obtained for the HOMP and HETP model are identical, so that figure 6(a) still holds for the HETP model. This is so because the critical densities do not depend on the values of k_1 and k_2. That further illustrates one point already mentioned in our discussion of n-alkane models. The presence of a maximum in the critical density for a chain model does not depend on differences in energy between terminal and interior sites.

The behaviour of the critical pressure for the HETP model is shown in figure 7. By comparing figure 6(b) and figure 7 it can be seen that the region of monotonic decay for the pressure (labelled as 1) is now much larger. The maximum in the critical pressure (regions 2, 3, 4 ...) appears now in a smaller region of the c_1, c_2 space (i.e., less types of chains are able to exhibit a maximum in the critical pressure). For a given value of c_1 and c_2, the maximum in the critical pressure is shifted to considerably shorter chains in the HETP model when compared to the HOMP model. Obviously, for sufficiently large values of k_1 and k_2, no maximum in the critical pressure would appear at all and the region labelled as 1 would dominate the whole c_1, c_2 space.

The choice of the maximum allowed values of c_1 and c_2 presented in figures 6 and 7 deserves some discussion. Obviously, the maximum allowed value of c_2 is $\pi/6$ (i.e., the addition of a monomer increases the volume by $\pi/6$ at most). We mentioned that c_2 can be related approximately to L^*. Therefore, for each value of c_2 (i.e., L^*), the maximum value of the parameter c_1 must be determined. For each value of c_2 (i.e., L^*), the maximum increase in α (or from equation (29) in m), and therefore the maximum

value of c_1, is obtained when we are considering a chain of rigid spheres in a linear configuration. For rigid linear chains, the slope of the plot of α versus n is given approximately by

$$c_1^{\max} = L^{*2}/(3L^* - L^{*3}). \tag{33}$$

Therefore, for a given value of c_2 (i.e., L^*), the maximum value of c_1 is given by equation (33) (see the dashed line in figures 6 and 7). Note that for $L^* = 1$, $c_1^{\max} = 0{\cdot}5$, so that from equation (29) $m = n$.

The results presented so far lead to two interesting conclusions. The first is that the presence or absence of a maximum in the critical density can be determined from purely geometric arguments, namely from an evaluation of c_1 and c_2 for the considered model. The molecular shape is responsible for the presence or absence of a maximum in the critical density. The second is that in order to determine the presence or absence of a maximum in the critical pressure, the geometry (i.e., c_1, c_2) and the energy difference between extreme and interior sites should be considered.

Can we understand the origin of the maximum in the critical density on a simple basis? A simple explanation of the appearance of a maximum in the critical density is provided by equation (32) which after substitution of equation (28) can be rewritten as

$$d_c' = y_c(\alpha(n, c_1))\, d_s(n, c_2) \tag{34}$$

$$d_s = n/V_m = n/[\sigma^3(\pi/6 + (n-1)\, c_2)]. \tag{35}$$

If α (or m) grows continuously with n, y_c goes to zero as n goes to infinity. In fact, the only way y_c may reach a finite asymptotic value is that α reaches a finite asymptotic value when n goes to infinity, and this has not been found for any chain model. Therefore, the consequence of increasing α with n is the decrease of y_c. The geometric factor denoted as site density d_s is an increasing function of n and reaches a finite asymptotic value for large values of n. Therefore, when n goes to infinity, d_c' goes to zero. For moderate values of n, however, the product of a decreasing and an increasing function may yield either a maximum or a monotonic decay. The origin of the maximum in the critical density is the compromise between the decay of y_c with n and the increases of d_s with n. Within the united atom approach that we are using in this work (i.e., each monomer unit is represented by a single sphere), d_s is a constant for a model with no overlaps between bonded units. Therefore for a model without overlaps between bonded units there cannot be a maximum in the critical density. That is why continuum models with $L^* = 1$ cannot present a maximum in the critical density. The same holds for lattice models (where d_s does not depend on n), and therefore in a lattice model a maximum in the critical density cannot be achieved. Recent Gibbs ensemble simulations [50] seem to confirm this conclusion, which is consistent with the predictions of the Flory–Huggins theory [51]. It is also clear from equation (34) that lattice theories cannot be used for describing the existence of a maximum in the critical density of continuous models, since the overlapping between bonded spheres is a requirement for its existence.

Equation (34) summarizes the requirements for the existence of a maximum in the critical density. On the one hand, d_s must increase with n (within the united atom description this is equivalent to saying that there must be overlaps between bonded spheres). On the other hand, y_c must decrease slowly with n and this is achieved when the non-sphericity of the model does not increase too quickly with n. When L^* is small, y_c decreases slowly with n so that there is always a maximum, regardless of whether the molecule is rigid or flexible.

Equation (34) is valid when the masses of the monomer and the interior and exterior sites, m_m, m_i and m_e, respectively, are the same. When these masses are different, equation (34) can be rewritten as

$$d_c = y_c(\alpha(n, c_1)) f_m d_s(n, c_2), \tag{36}$$

$$f_m = m_T/(nm_i) = \delta_{n,1}(m_m/m_i) + (1 - \delta_{n,1})(2m_e/m_i + (n-2))/n, \tag{37}$$

where m_T is the total mass of the molecule. Our previous discussion assumed $f_m = 1$. If the masses m_m and m_e are much larger than m_i, f_m will decrease very quickly with n. In this case, the maximum in the critical density will be shifted to shorter chains and eventually, for very large values of m_m/m_i and m_e/m_i, the maximum will disappear. Therefore, an additional condition for the appearance of a maximum in the critical density is that the masses of the monomer and exterior sites do not differ much from that of an interior site. This is the case for n-alkanes and for most of chain molecules, where the ratios m_m/m_i and m_e/m_i do not differ significantly from unity.

Let us now present a simple explanation of the appearance of a maximum in the critical pressure. The critical pressure obtained from equation (26) or equation (31) can be written as

$$p_c/(\varepsilon_{i-i}/\sigma^3) = \frac{y_c(\alpha) Z_c(y_c(\alpha), \alpha)}{V_m^*} T_c^*, \tag{38}$$

where Z_c is the compressibility factor at the critical point. The reduced temperature T^* is defined as

$$T^* = T/(\varepsilon_{i-i}/k), \tag{39}$$

and therefore T_c^* is the reduced critical temperature. In Appendix B the equation for T_c^* is given (see equation (B 2)). By replacing the expression of T_c^* into equation (38) one obtains

$$p_c/(\varepsilon_{i-i}/\sigma^3) = 11{\cdot}608\,12 \left[f_\varepsilon \frac{y_c(\alpha) Z_c(y_c(\alpha), \alpha)}{(2Z_0'(y_c(\alpha), \alpha) + y_c Z_0''(y_c(\alpha), \alpha))} \right] [d_s]^2, \tag{40}$$

where Z_0' and Z_0'' stand for the first and second derivatives of Z_0 with respect to y and the function f_ε has been defined as

$$f_\varepsilon = \varepsilon_T/(n^2\varepsilon_{i-i}) = \delta_{n,1} k_1 + (1 - \delta_{n,1})(4k_2 + (n-2)^2 + 4(n-2)\sqrt{k_2})/n^2. \tag{41}$$

Let us first discuss equation (40) for the HOMP model, where $f_\varepsilon = 1$. The first term in brackets on the right-hand side decreases continuously with α. Since we assumed $c_1 > 0$, the first term in brackets on the right-hand side of equation (40) decreases with n. The function d_s, however, increases with n (except for the case $L^* = 1$). The product of a function which decreases with n and a function which increases with n may yield a maximum. As in the case for the critical density, if $L^* = 1$, d_s is independent of n and therefore no maximum in the critical pressure can exist. The same is true for a lattice model. Within the united atom description of chain molecules, the presence of a maximum in the critical pressure requires a certain amount of overlap between contiguous sites.

Let us now discuss the case of the HETP model with $k_1 = 3$ and $k_2 = 2$. In this case, f_ε (see equation (41)) is no longer equal to one but decreases with n. The larger k_1 with respect to k_2 (and k_2 with respect to one), the faster is the decrease of f_ε with n. Therefore, for the HETP model, the decrease with n of the first term in brackets on the right-hand side of equation (40) is fast. Hence, for a given value of L^* (which

determines the behaviour of d_s), the maximum in the critical pressure is shifted to shorter chains when compared with the HOMP model.

Now it has been shown clearly why the difference in energy between the monomer, exterior and interior sites affects considerably the location of the maximum in the critical pressure. Equations (36) and (40) are probably the crucial results of this work since they provide a neat and simple explanation of the appearance of maxima in the critical density or pressure of chain molecules.

Before leaving this discussion we would like to mention that the increases of d_s with n can also be achieved for models not following the united atom description. For instance in a recent work, Archer *et al.* [52] describe n-alkanes as a set of n tangent hard spheres (which mimic the carbon atoms) and a set of $2n+2$ hard spheres tangent to the carbons (which mimic the hydrogen atoms) (see figure 1 (*d*) of [52]). The function d_s for such a model is given (for $n > 1$) by

$$d_s = (n)/(nV_C + (2n+2)\, V_H), \tag{42}$$

where V_C and V_H are the volumes of the hard spheres describing the carbon and hydrogen atoms, respectively. It is clear from equation (42) that in the model of Archer *et al.*, d_s is also an increasing function of n. Therefore the model of Archer *et al.* could present maxima in critical density or pressure. In fact Archer *et al.* have predicted the existence of a maximum in the critical pressure for their model [52]. The purpose of this digression is to illustrate that the general condition for the existence of maxima in critical density or pressure is the increase of d_s (the ratio between the number of monomer units of the chain and the total volume). In the united atom description, that requires overlaps between monomer units, but in the model of Archer *et al.* the increase of d_s with n does not require overlaps between the constituting atoms.

The results presented so far provide a general view of the variation of the critical properties of chain molecules with the number of monomer units. Our discussion on the variation of critical properties with n was established in terms of the parameters c_1 and c_2. However, it is difficult to visualize what set of c_1, c_2 parameters correspond to a given chain.

In order to clarify in more detail the geometrical requirements that favour the presence of maxima in critical properties, we shall proceed as follows. The vapour–liquid equilibria will be computed directly from equation (24) for the following models:

(i) The monomer:
(ii) dimers with different bond lengths L^*;
(iii) trimers with different bond lengths L^*, and bond angles θ;
(iv) tetramers with different bond lengths L,* bond angles θ, and differing in flexibility. For each tetramer (with a given value of L^* and θ) two kind of models will be considered. The fully rigid model (FR), in which it is supposed that $D = \infty$, and the fully flexible (FF), in which $D = 0$. The non-sphericity of the FR tetramers, α_{FR}, and FF tetramers, α_{FF}, are given by

$$\alpha_{FR}(n = 4) = \alpha_{trans} \tag{43}$$

$$\alpha_{FF}(n = 4) = 1/3\alpha_{trans} + 2/3\alpha_{gauche} \tag{44}$$

where α_{trans} and α_{gauche} are the non-sphericities of the *trans* and *gauche* conformers, respectively. Similar equations to (43) and (44) can be written for the volume of the FR and FF tetramers.

Table 4. Volume, V_m, and non-sphericity parameter, α, for some triatomic and tetraatomic models; n is the number of monomers, L^* the reduced bond length and θ the internal angle between monomers. The volume is given in units of d^3 where d is the diameter of the hard sphere associated to each interaction site. In the case of $n = 4$, results are provided for the *trans* conformer ($\phi = 0°$) and for the *gauche* conformer ($\phi = 120°$).

n	L^*	θ/degree	ϕ/degree	V_m/d^3	α
3	0·4	90	*	1·0950	1·1140
3	0·6	90	*	1·3476	1·2679
3	1·0	90	*	1·5708	1·8535
3	0·4	130	*	1·1184	1·1635
3	0·6	130	*	1·3530	1·3383
3	1·0	130	*	1·5708	1·9531
3	0·4	180	*	1·1184	1·1798
3	0·6	180	*	1·3530	1·3622
3	1·0	180	*	1·5708	2·0000
4	0·4	90	0	1·3690	1·1760
4	0·4	90	120	1·3340	1·1234
4	0·6	90	0	1·7569	1·3956
4	0·6	90	120	1·7439	1·3039
4	1	90	0	2·0944	2·2069
4	1	90	120	2·0944	2·085
4	0·4	130	0	1·4157	1·2703
4	0·4	130	120	1·4157	1·2519
4	0·6	130	0	1·7677	1·5291
4	0·6	130	120	1·7677	1·5010
4	1	130	0	2·0944	2·4061
4	1	130	120	2·0944	2·3496
4	0·4	180	0	1·4158	1·3017
4	0·4	180	120	1·4158	1·3017
4	0·6	180	0	1·7677	1·5757
4	0·6	180	120	1·7677	1·5757
4	1	180	0	2·0944	2·5
4	1	180	120	2·0944	2·5

(v) The vapour–liquid equilibria will be computed for $n = 5$ and $n = 6$ for the FF and FR models. To estimate α and V_m for the FF model with $n = 5, 6$, we shall simply assume that a linear extrapolation of the results of α and V_m for $n = 3$ and $n = 4$ provides reasonable results.

For models (i) to (iii) and for the *trans* and *gauche* conformers of model (iv), α will be estimated by using equation (15) along with the procedure proposed by Alejandre *et al.* [53] for estimating R_m. The molecular volume of all these models will be computed exactly with the procedure of Dodd and Theodorou [54]. Values of α and V_m are presented in table 4.

Once the vapour–liquid equilibria of the models described in points (i) to (v) have been computed, the critical densities are obtained from equation (32) (we shall assume $f_m = 1$). For each value of L^*, θ and D, which define the geometry of the chain, we analyse for which n-mer a maximum appears in the critical density. Steps (i) to (v) define the geometry of the chain. A full description of the chain also requires the ratio of the interaction energies between monomer, exterior and interior sites, defined by the parameters k_1 and k_2. We shall compute the vapour–liquid equilibria for the geometries described by steps (*a*) to (*e*) for the HOMP model with $k_1 = k_2 = 1$.

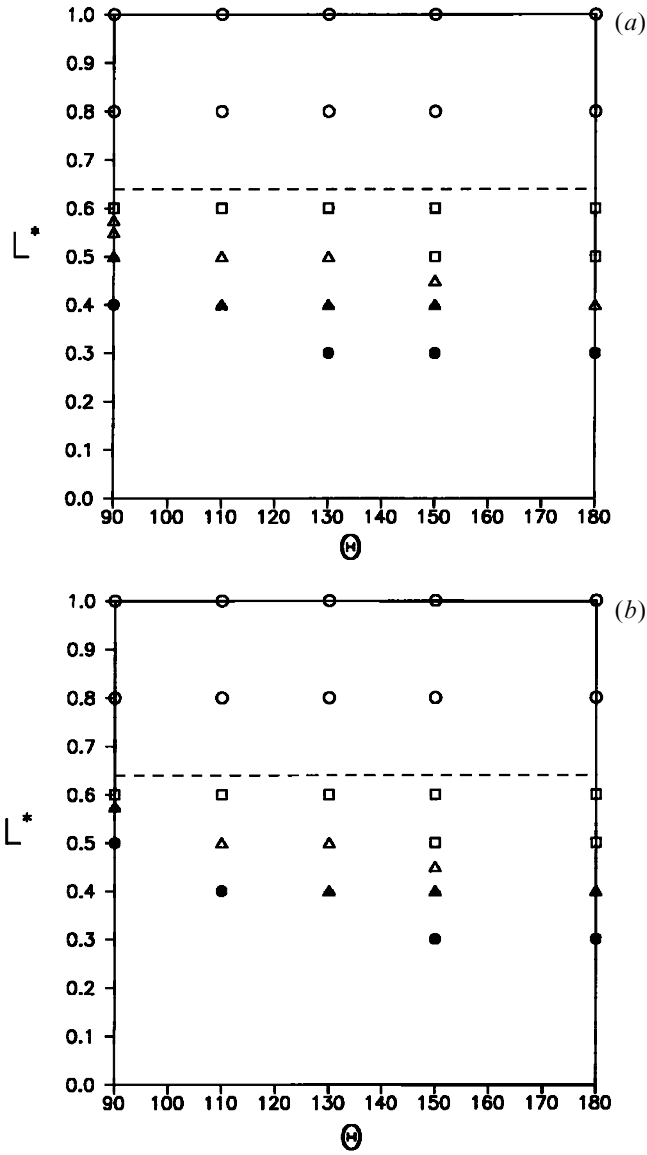

Figure 8. Regions where the maximum in the critical density for the HOMP model appears in the monomer (open circles), in the dimer (open squares), in the trimer (open triangles), in the tetramer (filled triangles) or in the hexamer (filled circles). The dashed curve separates the region where the maximum in the critical density appears in the monomer from the region where it appears in the dimer. (*a*) Results for the FR model; (*b*) results for the FF model.

Figure 8(*a*) shows the results for the FF model and figure 8(*b*) those for the FR model. In figure 8 each symbol corresponds to a different *n*-mer, and its location in the L^* versus θ plot shows the region where the maximum in d_c^* occurs for that particular *n*-mer. A plot equivalent to that presented in figure 8 can be drawn for the critical pressure of the HOMP chain. Since the pressure diagram is almost identical to that presented in figure 8 for the critical density, it will not be shown here. Thus, the

conclusions which follow can also be applied to the pressure. From the results presented in figure 8, the following conclusions for HOMP chains can be obtained:

(1) The maximum in the critical density (pressure) appears in the monomer regardless of the bonding angle, when $L^* > 0{\cdot}64$ (or $L^* > 0{\cdot}61$ in the case of the critical pressure).
(2) Any chain built with tangent spheres (i.e., $L^* = 1$) will present a maximum in the critical density (pressure) for the monomer. A certain degree of overlap between the bonded spheres is required in order to have the maximum in the critical density (pressure) in an n-mer different from the monomer.
(3) For chains with the bond angle $\theta = 90°$, the maximum in the critical density appears in the dimer for elongations between $L^* = 0{\cdot}64$ and $L^* = 0{\cdot}59$. When the bond angle is $\theta = 180°$, the maximum in the critical density appears in the dimer when the elongation is between the values $L^* = 0{\cdot}64$ and $L^* = 0{\cdot}45$.
(4) By comparing figure 8(a) and figure 8(b), it is seen that the presence of flexibility (i.e., a low value of D) shifts the maximum to longer chains for a given L^* and θ.
(5) The maximum in the critical density appears in the pentamer or hexamer only when L^* is less than 0·5.

In this section a rather extensive discussion of the variation of critical properties for short chains has been given. Is there any evidence supporting the conclusions presented in this work? Now, we shall compare the predictions presented in figure 8 with computer simulation data.

The Gibbs ensemble methodology [8] has been so far applied to three different kinds of chains, so that their critical properties are now available. The M1 model consists of a rigid linear chain with $L^* = 1$ and $\theta = 180°$, interacting through the LJ potential. For the M1 model, simulation results are available [55–58] for $n = 1$ and $n = 2$. The M2 model corresponds to a fully flexible chain with $L^* = 1$, the so-called pearl necklace model. Although it has no fixed bonding angle, geometrical considerations restrict it between $\theta = 60°$ and $\theta = 180°$. At low densities, where all bonding angles present the same probability, the average bonding angle is 107°. Therefore, we shall regard the M2 model as one presenting $L^* = 1$ and $\theta = 107°$. The third model (M3) corresponds to an n-alkane with $L^* = 0{\cdot}40$ and $\theta = 110°$. For the M2 model, no maxima have been found in the computer simulation [59, 60] results, neither for the critical density nor for the pressure and this is in agreement with the results presented in figure 8. For Gibbs ensemble results of the M3 model, a maximum was found in the critical density [7] and this is in agreement with the results of figure 8. By analysing the results of the M1 model presented in [55–58], it can be concluded that the critical density of the dimer is larger than that of the monomer for $L^* < 0{\cdot}78$ and that the critical pressure of the dimer is larger than that of the monomer for $L^* < 0{\cdot}70$. Our figure 8 shows that in the theory of this work the density of the dimer is larger than that of the monomer for $L^* < 0{\cdot}64$ and that the critical pressure of the dimer is larger than that of the monomer for $L^* < 0{\cdot}61$. Although the theory of this work is not quantitatively correct (the maximum elongation needed for the critical density or pressure of the dimer to be higher than that of the monomer is predicted with an error of 20%), it predicts correctly the existence of such a maximum elongation. The difference between the theoretical and simulation results for this maximum value of L^* is due to the use of the mean-field approximation within the theory. Although the use

of this approximation prevents quantitative predictions, we believe that the picture emerging from the results presented in this work is qualitatively correct.

5. Conclusions

In this work the vapour–liquid equilibria of n-alkanes modelled within the united-atom approach have been computed from perturbation theory. The reference system containing the repulsive forces is described by using a very accurate EOS recently proposed. Attractive forces are treated within the mean-field approximation. Intramolecular contributions to the free energy are assumed to be constant with density, so that they are neglected in the vapour–liquid equilibrium calculations. Two models were considered, one in which the CH_4, CH_3 and CH_2 differ in the interaction energy, and another in which all have the same interaction energy. From the results of this work the following two conclusions can be obtained for the critical properties of n-alkanes:

(1) The critical density of n-alkanes can be correctly described by the simple perturbation theory proposed in this work. Neither the differences in interaction energy between CH_4, CH_3 and CH_2 nor the small differences in mass are responsible for the existence of a maximum in the critical density of n-alkanes.
(2) The critical pressure of n-alkanes can be correctly described by the simple perturbation theory proposed in this work. To explain the presence of a maximum in the critical pressure for ethane it is necessary to incorporate within the theory differences in interaction energy between CH_4, CH_3 and CH_2 groups. If the energy interactions between these groups is set to the same value, a maximum in the critical pressure is still predicted but it is located at n-hexane.

Analysing the critical properties of chain models, the following conclusions were obtained:

(*a*) The conditions needed for the existence of a maximum in the critical density are:
(i) increase of d_s (the ration between the number of monomer units and the molecular volume) with n. Within a united-atom description of the chain this requires overlaps between contiguous sites;
(ii) not too large differences in mass between monomer, exterior and interior sites.
(*b*) The conditions needed for the existence of a maximum in the critical pressure are:
(i) increase of d_s with n. Within a united-atom description of the chain this requires overlaps between contiguous sites;
(ii) not too large differences in energy interaction between the monomer, exterior and interior sites.
(*c*) The presence of flexibility is not a requirement for the existence of maxima in the critical density or pressure and, in fact, the existence of these maxima is expected even for rigid models.
(*d*) The maximum in the critical density or pressure is shifted to longer chains for short bond lengths, for small bond angles (i.e., close to the value 90°) and when the molecules present flexibility.

(*e*) Assuming that the molecular volume and anisotropy of chain molecules increases linearly with the number of monomer units, the theory of this work predicts that critical density and pressure go to zero for infinitely long chains. The theory of this work also predicts that the critical temperature and the compressibility factor at the critical point tends to a finite value for infinitely long chains.

The present treatment, although too simple to provide quantitative predictions, yields a general view of the main features present in the vapour–liquid equilibria of short-chain models.

This work has been financed by Project PB94-0285 of the DGICYT. We thank Dr Jackson for sending a preprint of [52] prior to publication and to Dr Dodd and Dr Theodorou for sending us their code for the evaluation of the volume and surface of an arbitrary polymer.

Appendix A

In this appendix we present a brief account of the procedure used to obtain the EOS of the WCA reference system described in section 2. We refer the reader to [35] for further details. To compute α, equation (15) is used and R_m was approximated as that of a hard parallelepiped with the same principal moments of inertia as the considered conformer. The values of S_m and V_m of each conformer were evaluated using the algorithm proposed by Dodd and Theodorou [54]. To obtain the value of α and V_m of the n-alkane, a Monte Carlo simulation of an isolated chain is performed, so that the non-sphericity parameter and volume are computed for each of the conformers appearing in the run. The values of α and V_m for the n-alkane are taken to be the resulting Monte Carlo averages.

To compute the volume of a given conformer, a hard sphere was assigned to each interaction site according to the Barker and Henderson [49] prescription (recall that our reference system is of the WCA type). In the HETA model, the diameter of the hard spheres assigned to the CH_4, CH_3 and CH_2 groups are different, whereas in the HOMA they are equal. Diameters d_{BH} obtained from the BH prescription were fitted to the following empirical expression:

$$T^* = T/(\varepsilon/k), \tag{A 1}$$

$$d_{BH}/\sigma = 1{\cdot}015\,35 - 3{\cdot}798\,55 \times 10^{-2} \ln(T^*) - 2{\cdot}876\,44 \times 10^{-3} (\ln(T^*))^2. \tag{A 2}$$

To obtain the diameter of CH_4, the value of ε for the CH_4–CH_4 interaction was used. The values for CH_3 and CH_2 were determined correspondingly.

The values of α and V_m were obtained for the HETA and HOMA models at T = 180, 366·88, 700, 1000, 1500 and 2000 K for n = 4, 6, 8, 12, 16, 30, 50 (i.e., n is the number of carbons of the n-alkane). For n = 1, the values of α and V_m/d_{BH}^3 are 1 and $\pi/6$, respectively. For n = 2, α is obtained from equation (15) by using R_m of the corresponding spherocylinder. The values of α and V_m/d_{BH}^3 obtained for n = 1, 2, 4, 6, 8, 12, 16, 30, 50 were fitted to the following empirical formulae:

$$T_r = T/(49{\cdot}7\ \mathrm{K}), \tag{A 3}$$

$$\alpha = (a_1 + a_2 T_r + a_3 T_r^2 + a_4 T_r^3) + (a_5 + a_6 T_r + a_7 T_r^2 + a_8 T_r^3)\, n + (a_9 + a_{10} T_r + a_{11} T_r^2 + a_{12} T_r^3)\, n^2 + (a_{13} + a_{14} T_r + a_{15} T_r^2 + a_{16} T_r^3)\, n^3, \tag{A 4}$$

$$V_m/\sigma^3 = (d_{BH}/\sigma)^3 ((\nu_1 + \nu_2 T_r + \nu_3 T_r^2 + \nu_4 T_r^3) + (\nu_5 + \nu_6 T_r + \nu_7 T_r^2 + \nu_8 T_r^3)\, n). \tag{A 5}$$

Table 5. Coefficients a_1–a_{16} and ν_1–ν_8 of equations (A 4) and (A 5). These coefficients are used to obtain the EOS of repulsive WCA n-alkane chains. The coefficients of the fitting for the HETA and HOMA n-alkane models are provided here.

Coefficient	HOMA	HETA
a_1	$9{\cdot}05091\times10^{-1}$	$9{\cdot}05151\times10^{-1}$
a_2	$-1{\cdot}77866\times10^{-3}$	$-1{\cdot}52156\times10^{-3}$
a_3	$5{\cdot}61127\times10^{-5}$	$4{\cdot}17945\times10^{-5}$
a_4	$-5{\cdot}78171\times10^{-7}$	$-4{\cdot}16278\times10^{-7}$
a_5	$7{\cdot}19401\times10^{-2}$	$6{\cdot}9869\times10^{-2}$
a_6	1.77613×10^{-3}	$1{\cdot}56429\times10^{-3}$
a_7	$-4{\cdot}812\times10^{-5}$	$-3{\cdot}87197\times10^{-5}$
a_8	$4{\cdot}87893\times10^{-7}$	$3{\cdot}63132\times10^{-7}$
a_9	$1{\cdot}69681\times10^{-3}$	$1{\cdot}8082\times10^{-3}$
a_{10}	$-1{\cdot}45712\times10^{-4}$	$-1{\cdot}33793\times10^{-4}$
a_{11}	$4{\cdot}91993\times10^{-6}$	$4{\cdot}10138\times10^{-6}$
a_{12}	$-5{\cdot}28644\times10^{-8}$	$-3{\cdot}99774\times10^{-8}$
a_{13}	$-2{\cdot}17643\times10^{-5}$	$-2{\cdot}28477\times10^{-5}$
a_{14}	$1{\cdot}46437\times10^{-6}$	$1{\cdot}32376\times10^{-6}$
a_{15}	$-4{\cdot}91707\times10^{-8}$	$-4{\cdot}08466\times10^{-8}$
a_{16}	$4{\cdot}89034\times10^{-10}$	$3{\cdot}87973\times10^{-10}$
ν_1	$2{\cdot}37517\times10^{-1}$	$2{\cdot}78713\times10^{-1}$
ν_2	$-1{\cdot}92082\times10^{-3}$	$-1{\cdot}00444\times10^{-3}$
ν_3	$1{\cdot}69782\times10^{-5}$	$1{\cdot}89791\times10^{-5}$
ν_4	$3{\cdot}65885\times10^{-8}$	$-1{\cdot}56057\times10^{-7}$
ν_5	$2{\cdot}85145\times10^{-1}$	$2{\cdot}87169\times10^{-1}$
ν_6	$3{\cdot}14031\times10^{-3}$	$2{\cdot}85922\times10^{-3}$
ν_7	$-7{\cdot}97876\times10^{-5}$	$-6{\cdot}10327\times10^{-5}$
ν_8	$8{\cdot}38226\times10^{-7}$	$5{\cdot}27893\times10^{-7}$

Values of the coefficients a_1–a_{16} and ν_1–ν_8 for the HETA and HOMA models are given in Table 5. The EOS for the WCA reference system is given by equation (10) with α and V_m obtained from equations (A 1) to (A 5).

Appendix B

In this appendix some features of the critical properties of chain molecules resulting from equation (26) will be determined. In particular, the asymptotic values of y_c and Z_c when $\alpha\to\infty$ and of T_c when $n\to\infty$ will be evaluated. Equation (26) can be rewritten as:

$$p/(kT/\sigma^3) = yZ_0(y,\alpha)/(V_m^*) - 5{\cdot}80406 f_\varepsilon y^2/(T^*(V_m^*/n)^2). \tag{B 1}$$

By setting to zero the second derivative of equation (B 1) with respect to y, the critical temperature is obtained as:

$$T_c^* = 2f_\varepsilon \times 5{\cdot}80406 n^2/[V_m^*(2Z_0'(y_c,\alpha) + y_c Z_0''(y_c,\alpha))], \tag{B 2}$$

where $Z_0'(y_c,\alpha)$ and $Z_0''(y_c,\alpha)$ stand for the first and second derivatives of Z_0 with respect to y, evaluated at the critical packing fraction y_c. By setting to zero the first derivative of equation (B 1) with respect to y and using equation (B 2), y_c can be obtained by solving the following equation:

$$Z_0(y_c,\alpha) + y_c Z_0'(y_c,\alpha) - y_c(2Z_0'(y_c,\alpha) + y_c Z_0''(y_c,\alpha)) = 0. \tag{B 3}$$

As it can be seen from equation (B 3), y_c is a function of α only. The compressibility factor Z_c at the critical point can be obtained from equation (B 1) by substituting T^* by T_c^* from equation (B 2) and y by y_c. The final result is

$$Z_c = Z_0(y_c, \alpha) - (2Z_0'(y_c, \alpha) + y_c Z_0'')\, y_c/2. \tag{B 4}$$

Since y_c depends on α, Z_c depends only on α as well. In figure 5, y_c and Z_c are plotted as a function of α when using equation (10) for Z_0.

Let us now focus on the behaviour of y_c, T_c and Z_c when α goes to infinity. For that purpose let us write the virial expansion of Z_0 as

$$Z_0 = 1 + \sum_{i=2}^{\infty} B_i^* y^{i-1}, \tag{B 5}$$

where $B_i^* = B_i/V_m^{i-1}$ is the reduced ith virial coefficient of the reference system. When α goes to infinity, y_c tends to zero (see figure 5(*a*)). Therefore, for large values of α the virial expansion (equation (B 5)) can be truncated at second order in y without introducing much error. Replacing this truncated expansion in equation (B 3), one obtains

$$y_c^{\infty} = 1/(3B_3^*)^{1/2}, \tag{B 6}$$

where the superscript ∞ indicates that this expression is valid when α goes to infinity. If equation (10) is used for Z_0, equation (B 6) can be written as

$$y_c^{\infty} = 1/(43{\cdot}5\alpha)^{1/2}. \tag{B 7}$$

Let us now analyse the behaviour of Z_c^{∞}. Once Z_0 has been truncated at second order (correct for large values of α), equation (B 1) can be written as

$$Z_c = 1 + [B_2^* - 5{\cdot}804\,06 f_\varepsilon n^2/(V_m^* T^*)] y_c + B_3^* y_c^2. \tag{B 8}$$

The second term on the right-hand side of equation (B 10) tends to -1 for large values of α. This result can be easily derived by setting to zero the first derivative of equation (B 1) (truncated at second order in y) with respect to the packing fraction and using equation (B 6). Therefore, the first and the second term on the right-hand side of equation (B 8) cancel each other for large values of α and one obtains

$$Z_c^{\infty} = B_3^*(y_c^{\infty})^2 = 1/3, \tag{B 9}$$

where in the last equality we used the result of equation (B 6).

Finally, let us give the limit expression of the critical temperature. As it can be seen in equation (B 2), T_c^* is a function of n, V_m^* and α. Therefore, one cannot speak of the limit of T_c^* when α goes to infinity, since T_c^* is also a function of V_m^* and n. However, let us assume that we know V_m^* as a function of n and α as a function of n. Then, the limit of T_c^* when n goes to infinity, which will be denoted as T_c^{∞}, is given by (taking into account that f_ε tends to unity for very long chains):

$$T_c^{\infty} = 5{\cdot}804\,06/[(V^{\infty})^2((3b_3^{\infty})^{1/2} + b_2^{\infty})], \tag{B 10}$$

where we have defined

$$b_2^{\infty} = \lim_{n\to\infty} B_2^*/V_m^* \tag{B 11}$$

$$b_3^{\infty} = \lim_{n\to\infty} B_3^*/V_m^{*2} \tag{B 12}$$

$$V^{\infty} = \lim_{n\to\infty} V_m^*/n. \tag{B 13}$$

Equation (B 10) shows that within the theory described by equation (B 1), the critical temperature of an infinitely long chain (i.e., the theta temperature) remains finite if V^{∞} is not zero and at least one of the two b_i^{∞} terms (b_2^{∞} or b_3^{∞}) is different from zero. By using equation (10) for Z_0 and assuming that V_m^* and α are linear functions of n (see equations (27) and (28)), one obtains for T_c^{∞}:

$$T_c^{\infty} = 5{\cdot}804\,06/(3c_1c_2). \tag{B 14}$$

Two interesting conclusions can be obtained from equation (B 14). The first is that T_c^{∞} (i.e., the theta temperature of the polymer) decreases as L^* increases (see main text for the relation of c_2 with L^*). The second is that for a given value of L^* (i.e., c_2), a flexible model will have a higher value of T_c^{∞} than a rigid one, since c_1 will be lower for the former. (We are not considering here the possibility of liquid crystal formation which of course should be taken into account for rigid models with high anisotropy.)

References

[1] Reid, R. C., Prausnitz, J. M., and Poling, B. E., 1987, *The Properties of Gases and Liquids* (New York: McGraw-Hill).
[2] Ambrose, D., and Tsonopoulos, C., 1995, *J. chem. Engng Data*, **40**, 531.
[3] Smith, Jr., R, I., Teja, A. S., and Kay, W. B., 1987, *AIChE J.*, **33**, 232.
[4] Anselme, M. J., Gude, M., and Teja, A., 1990, *Fluid Phase Equilibria*, **57**, 317.
[5] Tsonopoulos, C., 1987, *AIChE J.*, **33**, 2080.
[6] Siepmann, J. I., Karaborni, S., and Smit, B., 1993, *Nature*, **365**, 330.
[7] Smit, B., Karaborni, S., and Siepmann, J. I., 1995, *J. chem. Phys.*, **102**, 2126.
[8] Panagiotopoulos, A. Z., 1987, *Molec. Phys.*, **61**, 813.
[9] Ryckaert, J. P., and Bellemans, A., 1978, *Faraday Discuss. chem. Soc.*, **66**, 95.
[10] Jorgensen, W. L., 1983, *J. Phys. Chem.*, **87**, 5304.
[11] Dickman, R., and Hall, C. K., 1988, *J. chem. Phys.*, **89**, 3168.
[12] Gao, J., and Weiner, J. H., 1989, *J. chem. Phys.*, **94**, 3168.
[13] Almarza, N. G., Enciso, E., Alonso, J., Bermejo, F. J., and Alvarez, M., 1990, *Molec. Phys.*, **70**, 485.
[14] Padilla, P., and Toxvaerd, S., 1991, *J. chem. Phys.*, **94**, 5650.
[15] Elliott, Jr., J. R., and Kanetkar, U. S., 1990, *Molec. Phys.*, **71**, 871.
[16] Yethiraj, A., 1995, *J. chem. Phys.*, **102**, 6874.
[17] Brown, D., Clarke, J. H., Okuda, M., and Yamazaki, T., 1994, *J. chem. Phys.*, **100**, 1684.
[18] Pratt, L. R., Hsu, C. S., and Chandler, D., 1978, *J. chem. Phys.*, **68**, 4202.
[19] Wertheim, M. S., 1987, *J. chem. Phys.*, **87**, 7323.
[20] Chapman, W. G., Jackson, G., and Gubbins, K. E., 1988, *Molec. Phys.*, **65**, 1057.
[21] Honnell, K. G., and Hall, C. K., 1989, *J. chem. Phys.*, **90**, 1841.
[22] Schweizer, K. S., and Curro, J. C., 1988, *J. chem. Phys.*, **89**, 3350.
[23] Boublik, T., 1989, *Molec. Phys.*, **66**, 191; see also Walsh, J. M., and Gubbins, K. E., 1990, *J. phys. Chem.*, **94**, 5115.
[24] Boublik, T., Vega, C., and Peña, M. D., 1990, *J. chem. Phys.*, **93**, 730.
[25] Chiew, Y. C., 1990, *Molec. Phys.*, **70**, 129.
[26] Amos, M. D., and Jackson, G., 1992, *J. chem. Phys.*, **96**, 4604.
[27] Sear, R. P., Amos, M. D., and Jackson, G., 1993, *Molec. Phys.*, **80**, 777.
[28] Phan, S., Kierlik, E., Rosinberg, M. L., Yu, H., and Stell, G., 1993, *J. chem. Phys.*, **99**, 5326.
[29] Thomas, A., and Donohue, M. D., 1993, *Ind. Engng chem., Res.*, **32**, 2093.
[30] Phan, S., Kierlik, E., and Rosinberg, M. L., 1994, *J. chem. Phys.*, **101**, 7997.
[31] Escobedo, F. A., and de Pablo, J. J., 1995, *J. chem. Phys.*, **103**, 1946.
[32] Costa, L. A., Zhou, Y., Hall, C. K., and Carra, S., 1995, *J. chem. Phys.*, **102**, 6212.
[33] Vega, C., Lago, S., and Garzón, B., 1994, *J. chem. Phys.*, **100**, 2182.
[34] Padilla, P., and Vega, C., 1995, *Molec. Phys.*, **84**, 435.
[35] Vega, C., MacDowell, L. G., and Padilla, P., 1996, *J. chem. Phys.*, **104**, 701.

[36] McQuarrie, D. A., 1976, *Statistical Mechanics* (New York: Harper & Row).
[37] Flory, P. J., 1969, *Statistical Mechanics of Chain Molecules* (New York: Wiley).
[38] Lopez Rodriguez, A., Vega, C., Freire, J. J., and Lago, S., 1993, *Molec. Phys.*, **80**, 1565.
[39] Lopez Rodriguez, A., Vega, C., Freire, J. J., and Lago, S., 1991, *Molec. Phys.*, **73**, 691.
[40] Weeks, J. D., Chandler, D., and Andersen, H. C., 1971, *J. chem. Phys.*, **54**, 5237.
[41] Rigby, M., 1976, *Molec. Phys.*, **32**, 575.
[42] Boublik, T., and Nezbeda, I., 1985, *Collect. Czech. chem. Commun.*, **51**, 2301.
[43] Kihara, T., 1963, *Adv. chem. Phys.*, **5**, 147.
[44] Attard, P., 1995, *J. chem., Phys.*, **102**, 5411.
[45] Almarza, N. G., Enciso, E., and Bermejo, F. J., 1992, *J. chem. Phys.*, **96**, 4625.
[46] Yethiraj, A., 1995, *J. chem. Phys.*, **102**, 6874.
[47] Jackson, G., and Gubbins, K. E., 1989, *Pure appl. Chem.*, **61**, 1021.
[48] O'Lenick, R., and Chiew, Y. C., 1995, *Molec. Phys.*, **85**, 257.
[49] Barker, J. A., and Henderson, D., 1976, *Rev. mod. Phys.*, **48**, 587.
[50] Mackie, A. D., Panagiotopoulos, A. Z., and Kumar, S. K., 1995, *J. chem. Phys.*, **102**, 1014.
[51] Flory, P. J., 1953, *Principles of Polymer Chemistry* (Ithaca, NY: Cornell University Press).
[52] Archer, A. L., Amos, M. D., Jackson, G., and McLure, I. A., 1996, *Int. J. Thermodyn. Phys.*, **17**, 201.
[53] Alejandre, J., Martinez-Casas, S. E., and Chapela, G. A., 1988, *Molec. Phys.*, **65**, 1185.
[54] Dodd, L. R., and Theodorou, D. N., 1991, *Molec. Phys.*, **72**, 1313.
[55] Lofti, A., Vrabec, J., and Fischer, J., 1992, *Molec. Phys.*, **76**, 1319.
[56] Dubey, G. S., O'Shea, S. F., and Monson, P. A., 1993, *Molec. Phys.*, **80**, 997.
[57] Galasi, G., and Tildesley, D. J., 1994, *Molec. Simulation*, **13**, 11.
[58] Kriebel, C., Muller, A., Winkelmann, J., and Fischer, J., 1995, *Molec. Phys.*, **84**, 381.
[59] Mooij, G. C. A. M., and Frenkel, D., 1994, *J. phys. Condensed Matter*, **6**, 3879.
[60] Sheng, Y. J., Panagiotopoulos, A. Z., Kumar, S. K., and Szleifer, I., 1994, *Macromolecules*, **27**, 400.
[61] Dymond, J. H., Cholinski, J. A., Szafranski, A., and Wyrzykowska-Stankiewicz, D., 1986, *Fluid Phase Equilibria*, **27**, 1.
[62] Yethiraj, A., Honnell, K. G., and Hall, C. K., 1992, *Macromolecules*, **25**, 3979.

Copyright © 2002 EBSCO Publishing